Ejected-electron spectroscopy of autoionizing resonances of helium excited by fast-electron impact

Zhe Zhang,[1,2] Xu Shan,[1,2] Enliang Wang,[1,2] and Xiangjun Chen[1,2,*]

[1]*Hefei National Laboratory for Physical Science at Microscale, University of Science and Technology of China, Hefei 230026, China*

[2]*Department of Modern Physics, University of Science and Technology of China, Hefei 230026, China*

(Received 26 March 2012; published 13 June 2012)

The autoionizing resonances $(2s^2)^1S$, $(2p^2)^1D$, and $(2s2p)^1P$ of helium have been investigated employing ejected-electron spectroscopy by fast-electron impact at incident energies of 250–2000 eV and ejected angles of 26°–116°. Shore parameters of the line shapes for these three resonances have been obtained in such high incident energy regime except at 250 eV. Distinct discrepancies between the present results at 250 eV and those of McDonald and Crowe at 200 eV [D. G. McDonald and A. Crowe, J. Phys. B **25**, 2129 (1992); **25**, 4313 (1992)] and Sise *et al*. at 250 eV [O. Sise, M. Dogan, I. Okur, and A. Crowe, Phys. Rev. A **84**, 022705 (2011)], especially for ^1D and ^1P states, are also observed.

DOI: 10.1103/PhysRevA.85.062702 PACS number(s): 34.80.Dp, 32.80.Zb

I. INTRODUCTION

Autoionization as the predominant decay channel of the doubly excited states of helium (He) has been attracting a lot of interest since the pioneering observations by Madden and Codling [1] in their photoabsorption experiment. The strong correlation between the two electrons [2] in the excitation-autoionization process of He generates a very sophisticated discrete line shape, called the "Fano" shape [3,4], embedded in the ionizing continuum region. If He is excited to the autoionizing states by electron impact, the autoionization will compete with the direct ionization as denoted:

$$\begin{aligned} e^-(\boldsymbol{k}_0) + \mathrm{He}(1s^2) &\rightarrow \mathrm{He}^{**}(nln'l') + e^-(\boldsymbol{k}_{\mathrm{sc}}) \\ &\rightarrow \mathrm{He}^+(1s) + e^-(\boldsymbol{k}_{\mathrm{ej}}) + e^-(\boldsymbol{k}_{\mathrm{sc}}) \\ &\quad \text{autoionization}, \qquad (1) \\ e^-(\boldsymbol{k}_0) + \mathrm{He}(1s^2) &\rightarrow \mathrm{He}^+(1s) + e^-(\boldsymbol{k}_{\mathrm{ej}}) + e^-(\boldsymbol{k}_{\mathrm{sc}}) \\ &\quad \text{direct ionization}, \end{aligned}$$

where $\boldsymbol{k}_0$, $\boldsymbol{k}_{\mathrm{sc}}$, and $\boldsymbol{k}_{\mathrm{ej}}$ are the momenta of the incident, scattered, and ejected electrons, respectively. It is clear that the final state of autoionization is completely indistinguishable from that of direct ionization. This degeneracy in energy leads to the interference between the amplitudes for the two processes. As a result, the asymmetric Fano profiles will be observed, which depends on not only the magnitudes but also the relative phases of the competing direct and resonant ionizing channels.

While Fano and co-workers [3,4] gave a theoretical analysis about the resonance profiles for photoabsorption and electron energy loss spectroscopy (EELS), a different kind of parametrization about the resonance profiles was derived by Shore [5] and Balashov *et al*. [6] and generalized by Tweed [7] for ejected-electron spectroscopy (EES). It has been proven that the shape parameters, either q of Fano shape or a and b of Shore-Balashov parametrization, which describes the interference between the direct ionization amplitude and the autoionization amplitude, are all sensitive to the dynamics and kinematics of the collision process. Therefore the measurements on autoionization of He not only provide a better understanding about the autoionization and electron-electron correlation, but are also an elaborate test of atomic collision theory.

In the last several decades, several kinds of electron-impact methods, such as EELS [8–11], EES [12–25], and $(e, 2e)$ coincidence spectroscopy [19,24–35], have been employed to observe the autoionization of He. In contrast to photoexcitation spectroscopy, the electron-impact technique is limited by low-energy resolution so that most of the experiments revealed only the doubly excited resonances below the He^+ $n = 2$ threshold. However, its unique advantage lies in the fact that it is possible to observe both the optically allowed and forbidden transitions [2].

EES, whose energy resolution is independent of the energy dispersion of the incident electron beam, is suitable for observing the autoionizing states which are closely spaced in energy. EES of the autoionizing states of He, the simplest multielectron atom, has long been investigated for several decades. Some of the studies [16,23] focused on the determination of the positions and widths of autoionizing states while others concentrated on the angular dependence of the line shapes of the four lowest-lying doubly excited resonant states—$(2s^2)^1S$, $(2s2p)^3P$, $(2p^2)^1D$, and $(2s2p)^1P$. Oda *et al*. [12,13,18] obtained a series of EES spectra corresponding to different incident energies (65–1000 eV) and ejected angles (13°–142°) as part of a comprehensive study about the energy and angular dependence of these resonant lines. However, only the angular dependence of Fano parameter q of the $(2s^2)^1S$ state at 250 eV incident energy was presented in their work [18]. EES spectra at different ejected angles were also obtained by Gelebart *et al*. [17] at 70, 80, and 100 eV incident energies and by Pochat *et al*. [19] at 100 eV. Shore-Balashov parametrization was used to analyze the spectra in both works. The results of the two studies had some differences while another experiment carried out by Moorehead and Crowe [25] supported Gelebart's results. The Shore parameters of the lowest-lying resonant states, except $(2p^2)^1D$, were calculated by Tweed and Langlois [36] (70 and 80 eV) and by Pochat *et al*. [19] (100 eV). Since only the first-order distorted wave model, including exchange, was used [37] and thus the direct ionizing amplitude could not be represented exactly [19], relatively poor agreement was achieved between the experimental and

*xjun@ustc.edu.cn

calculated results, except in the large angular region where autoionization contributes much more than direct ionization. In 1992, McDonald and Crowe [21,22] presented results in terms of Shore parameters concerning all four resonant states at 70, 80, 100, and 200 eV incident energies and 40°–130° ejected angles. The data showed disagreement with the data of Gelebart *et al*. [14], especially for small ejected angles. Recently, Sise *et al*. [24] published the angular dependence of Shore parameters of EES for $(2p^2)^1D$ and $(2s2p)^1P$ states at 250 eV. The disparities also appeared at small and large ejected angles for both parameters of the two states in comparison with the results of McDonald and Crowe [21] at 200 eV.

The discrepancies in angular variation of the shape parameters observed by EES for autoionization of He still exist after nearly 40 years since the early works by Gelebart *et al*. [14], both in experiments and in theoretical calculations. Therefore, it is worthwhile to continue this work and extend the parameters to higher incident energy, where the first-order calculation is generally regarded to be easily matched.

The present EES study has measured the $(2s^2)^1S$, $(2p^2)^1D$, and $(2s2p)^1P$ resonant states of He in a wide range of incident energies of 250–2000 eV and ejected angles of 26°–116°. The triplet state $(2s2p)^3P$, which is sited between the $(2s^2)^1S$ and $(2p^2)^1D$ states, is too weak to be observed at such high energies. The line shapes in the spectra corresponding to the three singlet resonant states have been analyzed in terms of Shore-Balashov parametrization; the angular and energy variations of the Shore parameters have been obtained and their features are described and discussed in detail.

II. THEORETICAL BACKGROUND

Assuming the autoionizing resonances with the same angular momentum and spin quantum numbers do not overlap, the double differential cross section (DDCS) of EES in the vicinity of the rth autoionizing resonances of He can be expressed in the parametrized form [5–7]:

$$\frac{d^2\sigma}{d\Omega_{\rm ej}dE_{\rm ej}} = f(\boldsymbol{k}_{\rm ej}) + \sum_{\mu}\frac{a_\mu(\boldsymbol{k}_{\rm ej})\varepsilon_\mu + b_\mu(\boldsymbol{k}_{\rm ej})}{1+\varepsilon_\mu^2}, \tag{2}$$

where

$$\varepsilon_\mu = 2(E_{\rm ej} - E_\mu)/\,\Gamma_\mu, \tag{3}$$

and $E_{\rm ej}$ and $\boldsymbol{k}_{\rm ej}$ are the energy and momentum, respectively, of the ejected-electron, while E_μ is the energy of the rth autoionizing resonance. The subscript μ, which is equal to $\{r; LMS\}$, denotes angular momentum and spin quantum numbers of the rth resonance. The full width at half maximum (FWHM) of resonance is indicated by Γ_μ.

The term f is the direct ionizing contribution to the DDCS in the vicinity of the resonances. The momentum-dependent Shore parameters a_μ and b_μ characterize the rth resonance. All of these parameters vary so slowly that they can be assumed to be constant in the energy region of the resonance. Additionally, they all have dimensions of DDCS and are given by [21,37]]

$$f(\boldsymbol{k}_{\rm ej}) = \frac{k_{\rm sc}}{k_0}\sum_S(2S+1)\int d\Omega_{\rm sc}\left|\sum_{LM}\boldsymbol{I}_\mu(\boldsymbol{k}_{\rm ej},\boldsymbol{K})\right|^2, \tag{4}$$

$$a_\mu(\boldsymbol{k}_{\rm ej}) = \frac{2k_{\rm sc}}{k_0}(2S+1)\int d\Omega_{\rm sc}{\rm Re}\sum_{\mu'}I^*_{\mu'}(\boldsymbol{k}_{\rm ej},\boldsymbol{K})\sum_M[\boldsymbol{J}_\mu(\boldsymbol{k}_{\rm ej},\boldsymbol{K})(\pi\boldsymbol{V}_{\boldsymbol{K}\mu})^{-1} - {\rm i}\boldsymbol{I}_\mu(\boldsymbol{k}_{\rm ej},\boldsymbol{K})], \tag{5}$$

$$\begin{aligned} b_\mu(\boldsymbol{k}_{\rm ej}) = {}& \frac{k_{\rm sc}}{k_0}(2S+1)\int d\Omega_{\rm sc}\left\{\left|\sum_M[\boldsymbol{J}_\mu(\boldsymbol{k}_{\rm ej},\boldsymbol{K})(\pi\boldsymbol{V}_{\boldsymbol{K}\mu})^{-1} - {\rm i}\boldsymbol{I}_\mu(\boldsymbol{k}_{\rm ej},\boldsymbol{K})]\right|^2\right\} \\ & + \frac{2k_{\rm sc}}{k_0}(2S+1)\int d\Omega_{\rm sc}{\rm Im}\sum_{\mu'}I^*_{\mu'}(\boldsymbol{k}_{\rm ej},\boldsymbol{K})\sum_M[\boldsymbol{J}_\mu(\boldsymbol{k}_{\rm ej},\boldsymbol{K})(\pi\boldsymbol{V}_{\boldsymbol{K}\mu})^{-1} - {\rm i}\boldsymbol{I}_\mu(\boldsymbol{k}_{\rm ej},\boldsymbol{K})], \end{aligned} \tag{6}$$

where momentum transfer $\boldsymbol{K}$ is given by $\boldsymbol{K} = \boldsymbol{k}_0 - \boldsymbol{k}_{\rm sc}$, and $d\Omega_{\rm sc}$ is the detected solid angle of the scattered electron. $\boldsymbol{I}_\mu$ and $\boldsymbol{J}_\mu$ are the direct and resonant ionizing amplitudes, respectively. $\boldsymbol{V}_{\boldsymbol{K}\mu}$ describes the transition from the excited state to the continuum.

It can be seen that expressions of both Shore parameters include an interference term between the direct and resonant ionization amplitudes, and the b_μ parameter has an additional term which is related to the pure resonant cross section. Hence, the a_μ parameter mainly describes the shape of the resonance profile, while the b_μ parameter mainly characterizes the resonance yield.

III. EXPERIMENTAL PROCEDURE

The apparatus used in this experiment is an $(e, 2e)$ spectrometer that has been described in detail elsewhere [38,39]. Some modifications have been made to fulfill the specific requirements of the present experiment. Instead of the electron gun with a hemispherical monochromator, which is designed for the high-resolution electron momentum spectroscopy experiments, an unmonochromized electron gun was employed to obtain higher intensity of the incident electron beam. Thus the relatively low-collision cross sections of the resonant excitations can be compensated, without affecting the energy resolution of EES. The gun can produce a well defined

TABLE I. The excitation energy E_L, natural width Γ_μ, and corresponding ejected-electron energy E_μ of autoionizing states of helium from the literature [34]. The value of 24.59 eV is used for the ionization energy ε to calculate E_μ.

	E_L (eV)	Γ_μ (eV)	$E_\mu = E_L - \varepsilon$ (eV)
$(2s^2)^1S$	57.84	0.120	33.25
$(2p^2)^1D$	59.91	0.057	35.32
$(2s2p)^1P$	60.15	0.038	35.56

electron beam with an energy range from about 250 to 2000 eV and a typical current of 0.5–2 μA. Only the slow electron detector unit was used in this EES experiment. The ejected electrons with energies ranging between 30 and 37 eV are gathered by a five-element electrostatic lens and then dispersed by the hemispherical analyzer. A position-sensitive detector, including two stacked microchannel plates (MCPs) followed by a resistive anode is mounted at the output of the analyzer. The energy of the detected electron is linearly related to the hitting position on the detector. Elastic scattering of He was employed to calibrate the energy-position relationship. The measured EES spectra have been put on the absolute energy scale by using the value of the ejected-electron energy of the ^1P state determined by the high-resolution experiments [34] (seen in Table I).

At each incident energy a series of spectra were measured from 26° to 116° at 10° intervals. The spectrum was accumulated at each angle in turn for an appropriate time to gain enough usable statistics. However, the experimental conditions, such as gas pressure, intensity of incident beam, etc., cannot be stably maintained over a long period of time so that the overall intensity of spectra obtained at different angles cannot be directly compared. A subsequent experiment, therefore, was performed, in which the angular distribution of the direct ionization cross sections was quickly measured over several scans in order to eliminate the drift. The obtained angular distribution was then used to calibrate the ejected-electron spectrometer at each angle, and the spectra can therefore be placed on a uniform cross-section scale.

For the sake of obtaining the angular-dependent relationships of Shore parameters of the $(2s^2)^1S$, $(2p^2)^1D$, and $(2s2p)^1P$ states at different incident energies, Eq. (2) convoluted with the instrumental function has been used to fit all the measured spectra by the least-squares method. The direct ionizing contribution f has been generally considered as a slowly varying function of $E_{\rm ej}$ in the energy range measured; it was found by deHarak *et al.* [23] that an empirical function $f = f_1 + f_2/E_{\rm ej}$, where f_1 and f_2 are constants for a given spectrum, showed an excellent description in the fitting. Thus it was also used in our fitting procedure. The E_μ and Γ_μ of the resonant states in the fitting are from high-resolution experiments [34] (seen in Table I). The FWHM of the Gaussian-type instrumental function has been set as a parameter to be determined by the fitting, since the observed widths of the resonant profiles measured at different conditions were found to be varied. The results of the fitting have revealed that the FWHM of instrumental function varies between about 100 and 200 meV.

IV. RESULTS AND DISCUSSIONS

A series of EES for the three resonant states, $(2s^2)^1S$, $(2p^2)^1D$, and $(2s2p)^1P$, have been measured and Figs. 1–3 show, as examples, the experimental spectra and the corresponding fitting at three incident energies of 250, 1000, and 2000 eV with ejected angles from 26° to 116°. It can be seen that the fitting spectra agree well with the experimental spectra at all incident energies and angles. The magnitudes and line shape asymmetries of the optically forbidden states, $(2s^2)^1S$ and $(2p^2)^1D$, both vary remarkably with the change of ejected angles while in the optically allowed state $(2s2p)^1P$ only the magnitude varies but the shape of the profiles is almost unchanged at all angles.

Direct ionization cross section f and the Shore parameters a and b of the $(2s^2)^1S$, $(2p^2)^1D$, and $(2s2p)^1P$ resonant states have been extracted by fitting the measured spectra at 250, 500, 1000, 1500, and 2000 eV incident energies. The angular variations of f at different incident energies are shown in Fig. 4. Along with the increasing of incident energy, the overall shape of angular variations of f remains unchanged, while the position of the maximum moves towards the larger angle. The angular variations of Shore parameters a and b

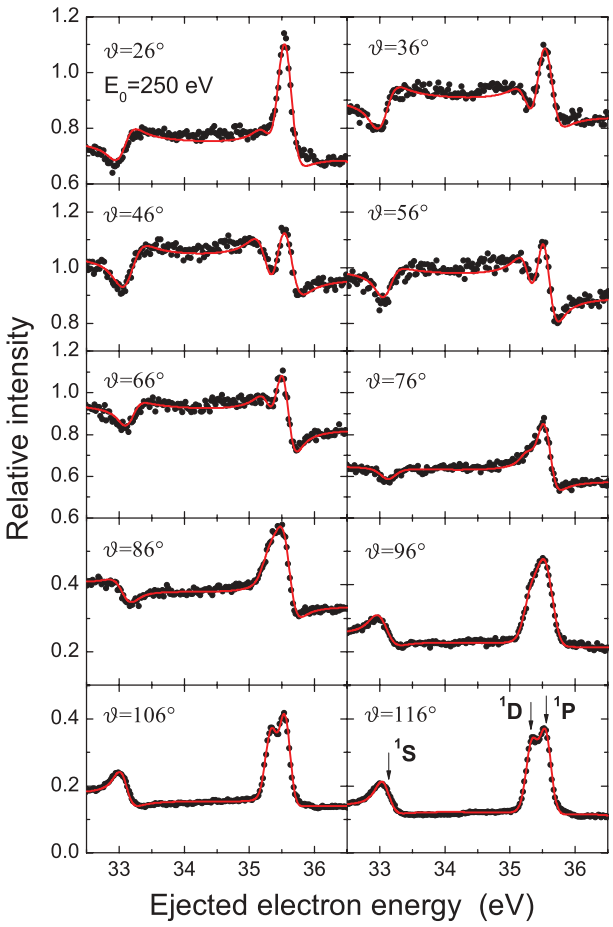

FIG. 1. (Color online) The ejected-electron spectra of helium at 250 eV incident energy for ejected angles from 26° to 116°. The solid circles indicate the spectra measured and the solid lines are the overall fit to the data.

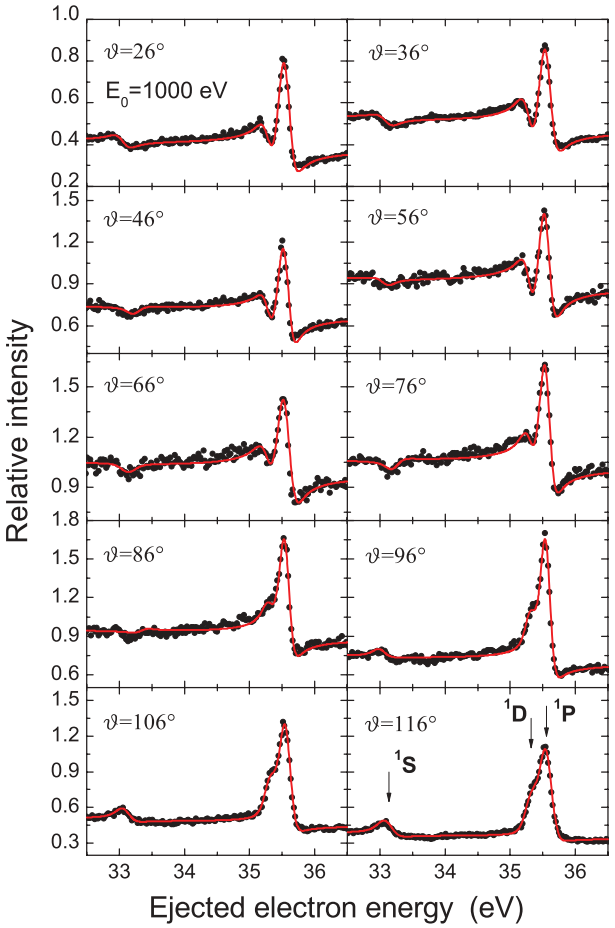

FIG. 2. (Color online) As in Fig. 1, except that the incident energy is 1000 eV.

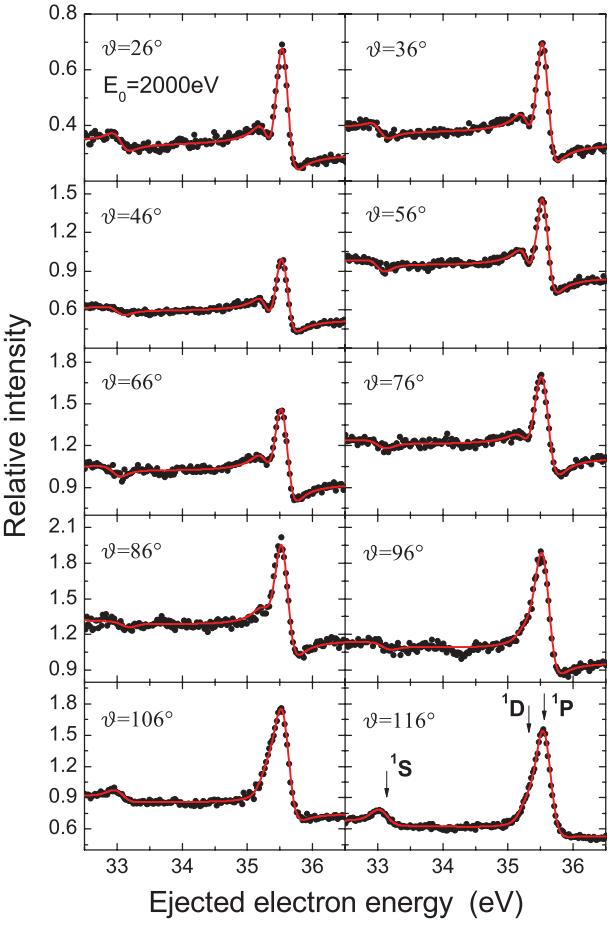

FIG. 3. (Color online) As in Fig. 1, except that the incident energy is 2000 eV.

of the three resonant states have been plotted in Figs. 5–7. The error bars shown in the figures for the present results are the uncertainties (one standard deviation) introduced in the fitting procedures. The only available experimental results of the Shore parameters of EES to be compared with the present data are from McDonald and Crowe [21,22] at 200 eV incident energy, and Sise *et al.* [24] at 250 eV. For the $(2p^2)^1D$ and $(2s2p)^1P$ resonant states, Sise *et al.*. have put their data and the data of McDonald and Crowe on the same scale in their paper [24], which seems to be achieved by normalizing the value of b at 60°. We rescaled our data by normalizing the direct ionization cross section f at each angle obtained at 250 eV to that of Sise *et al.*. Apparently, this operation completely eliminates the discrepancy of the detecting efficiency at different ejected angles between the experiments of Sise *et al.*. and ours. For the $(2s^2)^1S$ state, only the data of McDonald and Crowe [22] at 200 eV can be used for comparison. They did not publish the data of f so the above operation cannot be applied to put our data on the same scale as theirs. Thus only the maxima of the angular variations of the parameter a were simply rescaled to the same value and then the angular variations of parameter b were automatically placed on the same scale. Furthermore, the relative intensities of the present EES spectra at different incident energies have been rescaled by normalizing the maxima of the angular variations of parameter f. Therefore, the Shore parameters given here only describe the autoionizing resonance cross sections relative to the direct ionization cross sections at different incident energies.

In the case of $(2s^2)^1S$ resonance (Fig. 5), both parameters at 250 eV incident energy show fairly good agreement with that of McDonald and Crowe [22] at 200 eV. The a parameter at 250 eV descends along with the angles on the whole and there

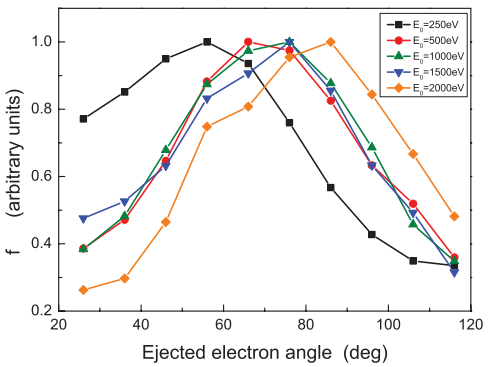

FIG. 4. (Color online) The direct ionization cross section f from the ejected-electron spectra of helium as a function of ejected angle at incident energies of 250 eV (black square), 500 eV (red circle), 1000 eV (green triangle), 1500 eV (blue downward triangle), and 2000 eV (orange diamond).

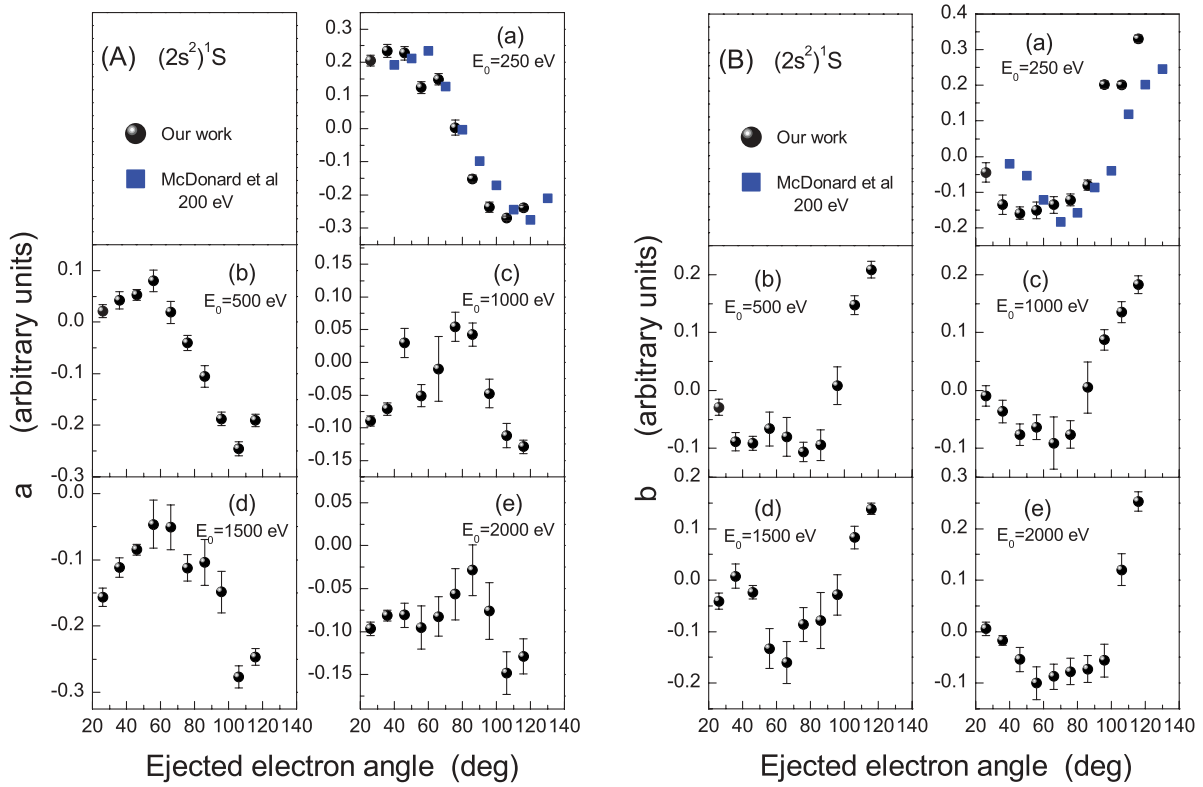

FIG. 5. (Color online) The Shore parameters a and b from the ejected-electron spectra as a function of ejected angle for the $(2s^2)^1S$ state of helium at incident energies (a) 250 eV, (b) 500 eV, (c) 1000 eV, (d) 1500 eV, and (e) 2000 eV.

are obviously oscillating trends at both small and large angles. There is a rounded minimum of the present angular variation of the b parameter in the vicinity of 60° while the minimum is much sharper at 70° for the results of McDonald and Crowe

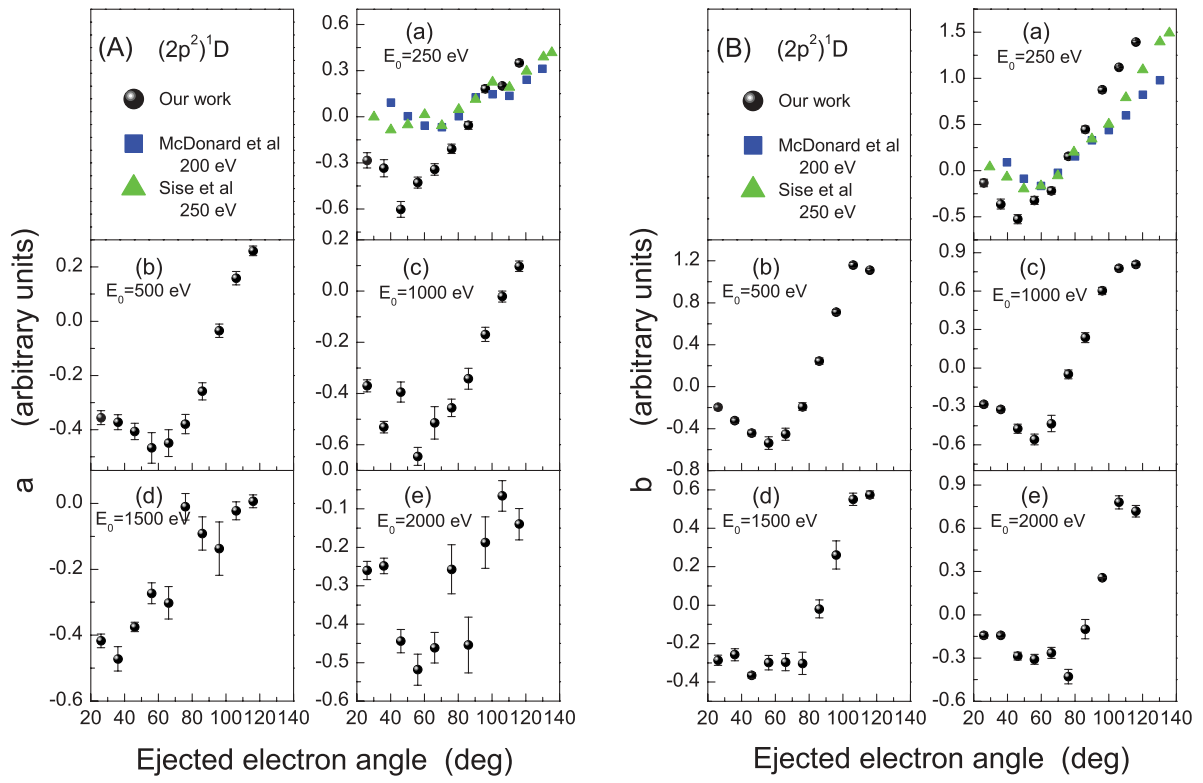

FIG. 6. (Color online) As in Fig. 4, but for the $(2p^2)^1D$ state of helium.

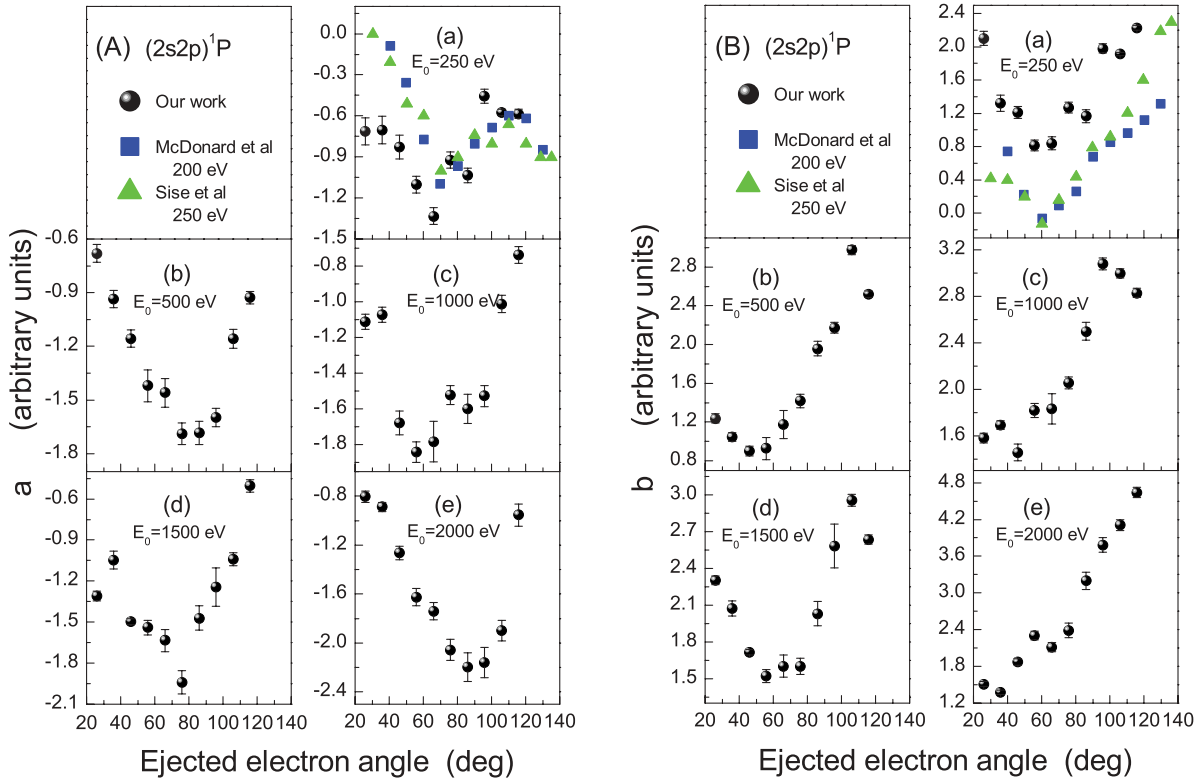

FIG. 7. (Color online) As in Fig. 4, but for the $(2s2p)^1P$ state of helium.

[22]. The phenomenon that the positions of the minima and maxima of both parameters of $(2s^2)^1S$ resonance move towards the larger angles as the incident energy is increased has been observed by McDonald and Crowe at incident energies of 70–200 eV. It is interesting that the trend continues in the present experiment at incident energies of 250–2000 eV. The position of the maximum of a moves from about 40° at 250 eV to about 90° at 2000 eV and the position of the minimum of a moves out of the angular range of ours ($\sim 116°$) after 500 eV. The angular variations of the b parameter reveal similar behavior at all incident energies, having a deep minimum around 40°–80° followed by a sharp increase at larger angles. In addition, McDonald and Crowe [22] pointed out that the value of the maximum of a as a function of angle varies from negative to positive as incident energy is increased from 70 to 200 eV, but the trend reverses as the incident energy is increased from 250 to 2000 eV, referring to our results that the value of maximum decreases from about 0.2 at 250 eV to about–0.05 at 2000 eV. At all incident energies the b parameter is negative in the forward direction and turns to positive in the backward. These behaviors result from strong interference. One can refer to the resonance shape of $(2s^2)^1S$ in Figs. 1–3. At 250 eV a dip occurs first at small angles where a is positive and it turns and becomes a window resonance at ∼76° where a is zero. At larger angles, where a is negative, the peak occurs first for the resonance. On the other hand, at higher incident energies, say 2000 eV, the peak occurs first at both small and large angles where a is negative, while it is more likely a window resonance at around 80° where a is close to zero.

For the $(2p^2)^1D$ and $(2s2p)^1P$ resonant states, steep oscillations of Shore parameters over the entire ejected angular range can be observed and the features of oscillation remain unchanged at every incident energy (Figs. 6 and 7). Distinct differences of the angular dependence of the parameters of the two states appear when comparing our results and those of Sise *et al*. (at incident energy of 250 eV) [24] and McDonald and Crowe (at 200 eV), especially for the $(2s2p)^1P$ state, where the b parameters of our study are obviously larger at all angles.

As shown in Fig. 6, the angular variations of both parameters of the $(2p^2)^1D$ state exhibit similar shapes at all incident energies. They all have the minima located at 46°–66°, except the curve for parameter a at 1500 eV whose minimum is at about 36°, with a value of about–0.5 to–0.6. The parameters a and b decrease slowly from 26° to the positions of the minima followed by a rapid increase at large angles in all cases. As in the case of the $(2s^2)^1S$ resonant state, the minima of the angular dependence of parameter a of the $(2s2p)^1P$ state move towards larger angles as the incident energy is increased (Fig. 7); this also continues the trend reported by McDonald and Crowe [21] from 70 to 200 eV. But the same trend cannot be observed in the present results of parameter b at higher incident energies. The values of minima of parameter a curves become more negative from–1.3 at 250 eV to–2.2 at 2000 eV while all the data remain negative at all incident energies. The parameter b of this resonance always keeps positive and grows from 2.0 to 4.5 with the increasing incident energy at large angles, or in other words, for the $(2s2p)^1P$ state the resonant ionization

dominates more in the backward direction as the incident energy is increased.

V. SUMMARY

The EES study for the autoionizing resonances of He in the region of the $(2s^2)^1S$, $(2p^2)^1D$, and $(2s2p)^1P$ states has been reported at higher incident energies of 250–2000 eV. The angular variations of the Shore parameters about the profile shapes of these resonances have been obtained in the ejected angular range of 26°–116° and reveal obvious oscillating features reflecting the interference between resonant and direct ionization amplitudes, which depends sensitively on both of the magnitudes and relative phases of the two amplitudes, i.e., the kinematical conditions of collision reaction and the symmetry of resonance itself [21]. The salient distinctions of the parameters of resonant line shapes between ours and Refs. [21,22,24] have been observed at low incident energy, especially for the $(2p^2)^1D$ and $(2s2p)^1P$ states. Therefore, besides further experimental studies, corresponding theoretical calculations are also absolutely essential. So far as we know, relative to the very few theoretical calculations about the DDCS of autoionization of He at low incident energy [19,36], many calculations have been developed for comparing and explaining the results of triple differential cross section (TDCS) of $(e, 2e)$ experiments about autoionization of He, such as the first-order distorted-wave model [19,36,40], six-state momentum space close-coupling approximation [41], and more sophisticated methods using the second-order theoretical model [33,34,42–45]. While first-order models reach a fair agreement in some cases, the second-order models have performed better in most cases. However, there are still some experimental results for which neither first- or second-order models cannot give a satisfactory description [33,34]. Hence, further understanding of autoionization dynamics is still desired. Although the momentum dependence of Shore parameters appears more sensitive at low incident energy, both the experimental and the theoretical considerations also become more complicated. Thus, it may be a good idea to reconsider the autoionization dynamics of He at a higher incident energy.

ACKNOWLEDGMENTS

This work was jointly supported by the National Basic Research Program of China (Grant No. 2010CB923301), the National Natural Science Foundation of China (Grants No. 10734040, No. 10979007), and the CAS knowledge promotion project (No. KJCX1-YW-N30).

[1] R. Madden and K. Codling, Phys. Rev. Lett. **10**, 516 (1963).
[2] G. Tanner, K. Richter, and J. M. Rost, Rev. Mod. Phys. **72**, 497 (2000).
[3] U. Fano, Phys. Rev. **124**, 1866 (1961).
[4] J. W. Cooper, U. Fano, and F. Prats, Phys. Rev. Lett. **10**, 518 (1963).
[5] B. W. Shore, J. Opt. Soc. Am. **57**, 881 (1967).
[6] V. V. Balashov, S. S. Lipovetskii, and V. S. Senashenko, Sov. Phys. JETP **36**, 858 (1973).
[7] R. J. Tweed, J. Phys. B **9**, 1725 (1976).
[8] S. M. Silverman and E. N. Lassettre, J. Chem. Phys. **40**, 1265 (1964).
[9] H. Wellenstein, R. Bonham, and R. Ulsh, Phys. Rev. A **8**, 304 (1973).
[10] X. W. Fan and K. T. Leung, J. Phys. B **34**, 811 (2001).
[11] X. J. Liu, L. F. Zhu, Z. S. Yuan, W. B. Li, H. D. Cheng, Y. P. Huang, Z. P. Zhong, K. Z. Xu, and J. M. Li, Phys. Rev. Lett. **91**, 193203 (2003).
[12] N. Oda, F. Nishimura, and S. Tahira, Phys. Rev. Lett. **24**, 42 (1970).
[13] N. Oda, F. Nishimura, and S. Tahira, J. Phys. Soc. Jpn. **33**, 462 (1972).
[14] F. Gelebart, R. J. Tweed, and J. Peresse, J. Phys. B **7**, L174 (1974).
[15] A. J. Smith, P. J. Hicks, F. H. Read, S. Cvejanovic, G. C. M. King, J. Comer, and J. M. Sharp, J. Phys. B **7**, L496 (1974).
[16] P. J. Hicks and J. Comer, J. Phys. B **8**, 1866 (1975).
[17] F. Gelebart, R. J. Tweed, and J. Peresse, J. Phys. B **9**, 1739 (1976).
[18] N. Oda, S. Tahira, F. Nishimura, and F. Koike, Phys. Rev. A **15**, 574 (1977).
[19] A. Pochat, R. J. Tweed, M. Doritch, and J. Peresse, J. Phys. B **15**, 2269 (1982).
[20] J. P. van den Brink, G. Nienhuis, J. van Eck, and H. G. Heideman, J. Phys. B **22**, 3501 (1989).
[21] D. G. McDonald and A. Crowe, J. Phys. B **25**, 2129 (1992).
[22] D. G. McDonald and A. Crowe, J. Phys. B **25**, 4313 (1992).
[23] B. A. deHarak, J. G. Childers, and N. L. S. Martin, Phys. Rev. A **74**, 032714 (2006).
[24] O. Sise, M. Dogan, I. Okur, and A. Crowe, Phys. Rev. A **84**, 022705 (2011).
[25] P. S. K. Moorehead and A. Crowe, in *Proceedings of the14th International Conference on the Physics of Electronic and Atomic Collisions* (Stanford University Press, Palo Alto, CA, 1985), p. 160.
[26] E. Weigold, A. Ugbabe, and P. J. O. Teubner, Phys. Rev. Lett. **35**, 209 (1975).
[27] J. Lower and E. Weigold, J. Phys. B **23**, 2819 (1990).
[28] D. G. McDonald and A. Crowe, Z. Phys. D **23**, 371 (1992).
[29] D. G. McDonald and A. Crowe, J. Phys. B **26**, 2887 (1993).
[30] A. Crowe, D. G. McDonald, S. E. Martin, and V. V. Balashov, Can. J. Phys. **74**, 736 (1996).
[31] M. J. Brunger, O. Samardzic, A. S. Kheifets, and E. Weigold, J. Phys. B **30**, 3267 (1997).
[32] O. Samardzic, L. Campbell, M. J. Brunger, A. S. Kheifets, and E. Weigold, J. Phys. B **30**, 4383 (1997).
[33] B. A. deHarak, K. Bartschat, and N. L. S. Martin, Phys. Rev. Lett. **100**, 063201 (2008).

[34] B. A. deHarak, K. Bartschat, and N. L. S. Martin, Phys. Rev. A **82**, 062705 (2010).
[35] O. Sise, M. Dogan, I. Okur, and A. Crowe, J. Phys. B **43**, 185201 (2010).
[36] R. J. Tweed and J. Langlois, J. Phys. B **19**, 3565 (1986).
[37] R. J. Tweed and J. Langlois, J. Phys. B **19**, 3583 (1986).
[38] X. J. Chen, X. Shan, and K. Z. Xu, in *Nanoscale Interactions and Their Applications: Essays in Honour of Ian McCarthy*, edited by F. Wang and M. J. Brunger (Transworld Research Network, Kerala, India, 2007), p. 37.
[39] X. Shan, X. J. Chen, L. X. Zhou, Z. J. Li, T. Liu, X. X. Xue, and K. Z. Xu, J. Chem. Phys. **125**, 154307 (2006).
[40] A. S. Kheifets, J. Phys. B **26**, 2053 (1993).
[41] I. E. McCarthy and B. Shang, Phys. Rev. A **47**, 4807 (1993).
[42] P. J. Marchalant, C. T. Whelan, and H. R. J. Walters, (Plenum, New York, 1997), pp. 21–43.
[43] Y. Fang and K. Bartschat, J. Phys. B **34**, L19 (2001).
[44] Y. Fang and K. Bartschat, J. Phys. B **34**, 2747 (2001).
[45] A. L. Godunov, J. H. McGuire, V. S. Schipakov, and A. Crowe, J. Phys. B **35**, L245 (2002).